

## Article

# 3-Mercaptopropanoic Acid-Doped Chitosan/Hybrid-Based Multilayer Sol-Gel Coatings for Cu Protection in 3.5% NaCl Solution

Jaganathan Balaji \* and Tae Hwan Oh \*

School of Chemical Engineering, Yeungnam University, Gyeongsan 38541, Korea

\* Correspondence: balajichem89@gmail.com (J.B.); taehwanoh@ynu.ac.kr (T.H.O.)

**Abstract:** In this work, biopolymer based sol-gel was synthesized by doping 3-mercaptopropanoic acid (MPA) with chitosan and a hybrid of 3-glycidoxypropyltrimethoxysilane (GPTMS) and tetraethoxysilane (TEOS). Prepared MPA/hybrid-doped chitosan was applied to a copper (Cu) metal surface by the self-assembly technique to protect the Cu metal from corrosion in a 3.5% NaCl solution. The structure, mechanism and morphology of the modified electrodes were examined using Fourier transform infra-red (FT-IR) spectroscopy, X-ray photoelectron spectroscopy (XPS), scanning electron microscopy (SEM) with energy-dispersive X-ray spectroscopy (EDX), and atomic force microscopy (AFM). The decrease in surface roughness for Hy/chitosan/MPA-coated Cu indicates the formation of a dense layer on Cu metal confirmed by AFM. The corrosion protection evaluation of sol-gel coated electrodes was analyzed using electrochemical impedance spectroscopy (EIS) and potentiodynamic polarization studies (PDS) in a 3.5% NaCl medium. The MPA/hybrid-doped chitosan sol-gel coated Cu metal showed the greatest resistance to corrosion than other sol-gel modified electrodes. The MPA-doped-chitosan/Hy sol-gel coating protected the Cu metal by an anodic dissolution process and improved its corrosion protection to 99.9%.

**Keywords:** copper; chitosan; hybrid; 3-mercaptopropanoic acid; 3.5% NaCl



**Citation:** Balaji, J.; Oh, T.H.

3-Mercaptopropanoic Acid-Doped Chitosan/Hybrid-Based Multilayer Sol-Gel Coatings for Cu Protection in 3.5% NaCl Solution. *Polymers* **2021**, *13*, 3743. <https://doi.org/10.3390/polym13213743>

Academic Editor: Yujie Qiang

Received: 28 June 2021

Accepted: 26 October 2021

Published: 29 October 2021

**Publisher's Note:** MDPI stays neutral with regard to jurisdictional claims in published maps and institutional affiliations.



**Copyright:** © 2021 by the authors. Licensee MDPI, Basel, Switzerland. This article is an open access article distributed under the terms and conditions of the Creative Commons Attribution (CC BY) license (<https://creativecommons.org/licenses/by/4.0/>).

## 1. Introduction

Copper (Cu) and its alloys exhibit virtuous electrical, mechanical, and antifouling properties, corrosion resistance, excellent thermal, and electrical conductivity and play a vital role in thermal coolant systems and electronics industries [1–3]. However, corrosion of Cu in seawater and chloride causes material and economic losses around the world [4–6]. Therefore, it is important that copper is protected from corrosion in aggressive chloride environments. As a result, the demand for much greener, non-toxic coatings for the protection of Cu metal is increasing [7].

Physical vapor deposition (PVD), chemical vapor deposition (CVD), plasma spraying, electrodeposition, and sol-gel coatings are the various coating strategies applied to the corrosion protection of the Cu metal [8]. Compared to other methods, sol-gel based coatings have a high ability to protect against corrosion through increased corrosion resistance due to their environmental friendliness, their excellent stability, and oxidation control [9,10]. Hybrid sol-gel coatings are the potential alternative to toxic current coatings like chromate and phosphate. Even though hybrid sol-gel coatings offer relatively dense films, some corrosive ions can still penetrate through the pores and corrode the copper metal. Thus, to overcome this disadvantage, the active biopolymer based on corrosion inhibitors can be incorporated into the sol-gel matrix for increased corrosion protection [11–13].

Chitosan, a biopolymer, has attracted many researchers and scientists due to its low cost, low toxicity, and environment-friendly nature, and has been used in a variety of medicinal applications [14]. Balaji et al. have studied hybrid zirconium and nano-TiO<sub>2</sub> doped coating with water soluble chitosan biopolymer as a corrosion inhibitor to

protect Al metals [15,16]. Several studies have reported on corrosion inhibitors as chitosan biopolymers for the protection of metal surfaces [17,18].

A self-assembled monolayer (SAM) is the formation of a dense film on Cu metal which acts as an effective barrier for corrosion protection [2]. Heterocyclic molecules of electron-rich compounds containing oxygen, nitrogen and sulphur can reinforce SAM on metallic surfaces. Cu metal is more attractive to mercapto (-SH) functionalized compounds and forms a barrier layer that protects the metallic surface from penetrating corrosive ions [19].

In this research, we performed laboratory-scale experiments that showed effective protection of the Cu metal in the 3.5% NaCl. The results showed an inhibition efficiency of 99.9% by using a sol-gel coating of 3-mercaptopropanoic acid (MPA), 3-glycidioxypropyltrimethoxysilane (GPTMS), and tetraethoxysilane (TEOS) hybrid chitosan biopolymer. The results show promise that this may be extended for the Cu metal used in the environment.

## 2. Materials and Methods

### 2.1. Chemicals

GPTMS with purity of 98%, TEOS with purity of 98%, chitosan, MPA with purity of 99%, sodium chloride (NaCl) with purity of 99%, and ethanol with purity of 99.5% were purchased from Sigma-Aldrich, Gangnam-Gu, Korea and used as received.

### 2.2. Cu Metal Polishing and Synthesis of Sol-Gel and Self-Assembly Coating

Cylindrical-shaped Cu metal electrode (a diameter of 1 cm) was polished using different grades of emery paper (1# to #7) and sonicated with acetone and ethanol for 30 min, and dried in a hot air oven. A hybrid (Hy) sol-gel matrix was prepared using ethanolic solutions of GPTMS and TEOS (2:1 molar ratio). This was stirred in a reaction vessel for 6 h and its pH was adjusted to 4.0 by adding HCl to promote hydrolysis and condensation reaction. Hy/chitosan was prepared by adding a chitosan solution (5 wt%) to hybrid sol in the molar ratio of 1:1 and continuously stirred for a further 6 h at 40 °C for a ring opening reaction. Then Hy/chitosan/MPA was prepared by adding MPA to Hy/chitosan sol (1:1 molar ratio) and continuously stirred for further 6 h at 40 °C for crosslinking. The polished Cu metal immersed in prepared Hy/chitosan/MPA sol-gel for 12 h. For comparative study polished Cu metal also immersed in Hy and Hy/chitosan sol-gel for 12 h. Then, the sol-gel coated Cu electrodes were dried in airflow at 80 °C for 2 h.

### 2.3. Characterization of Modified/Unmodified Cu Electrodes

The chemical composition of bare Cu, Hy coated, Hy/chitosan coated and Hy/chitosan/MPA coated Cu electrodes were examined using Fourier transform-infrared (FT-IR) spectra (Perkin Elmer Spectrum at Core Research Support Center for Natural Products and Medical Materials in Yeungnam University) and X-ray photoelectron spectroscopy was carried out using a K-Alpha spectrometer (Thermo Scientific, Waltham, MA, USA). The surface morphological analysis of modified and unmodified Cu electrodes were studied using field emission scanning electron microscopy (FESEM, Hitachi S-4800) and atomic force microscopy (AFM, Park system (XE 100) model).

The corrosion resistant efficiency of bare Cu, Hy-coated, Hy/chitosan-coated and Hy/chitosan/MPA-coated Cu electrodes were carried out using a CorrTest electrochemical workstation with conventional three-electrode set up. The electrochemical impedance spectroscopy (EIS) measurements were taken at the open circuit potential between the frequency ranges from 10 kHz to 0.01 Hz and the fitting results were obtained from ZSimpWin 3.21 software. The potentiodynamic polarization studies (PDS) were examined from  $-0.70$  V to  $0.2$  V vs. Ag/AgCl at the scan rate of  $1$  mV s<sup>-1</sup>.

### 3. Results and Discussion

#### 3.1. Fourier Transform Infrared (FT-IR) Analysis

The FT-IR spectra of Hy coated, Hy/chitosan coated, and Hy/chitosan/MPA coated Cu electrodes are shown in Figure 1. In the FT-IR spectra of the Hy coated electrode, the band at  $3434\text{ cm}^{-1}$ ,  $2949\text{ cm}^{-1}$ ,  $2890\text{ cm}^{-1}$ ,  $1728\text{ cm}^{-1}$ ,  $1645\text{ cm}^{-1}$ ,  $1425\text{ cm}^{-1}$  and  $1032\text{ cm}^{-1}$  are due to  $\text{-OH}$ ,  $\text{-CH}$  stretching,  $\text{C-C}$ , epoxy group and  $\text{Si-O-Si}$  bond formation [20–23]. Additionally, for the Hy/chitosan- and Hy/chitosan/MPA-coated electrodes, the additional bands at  $3402\text{ cm}^{-1}$  and  $1728\text{ cm}^{-1}$  are due to  $\text{-NH}$  stretching and  $\text{-NH}$  bending. The absence of  $\text{-SH}$  stretching at  $2632\text{ cm}^{-1}$  confirms the doping of chitosan and MPA in the hybrid sol-gel matrix [24,25].

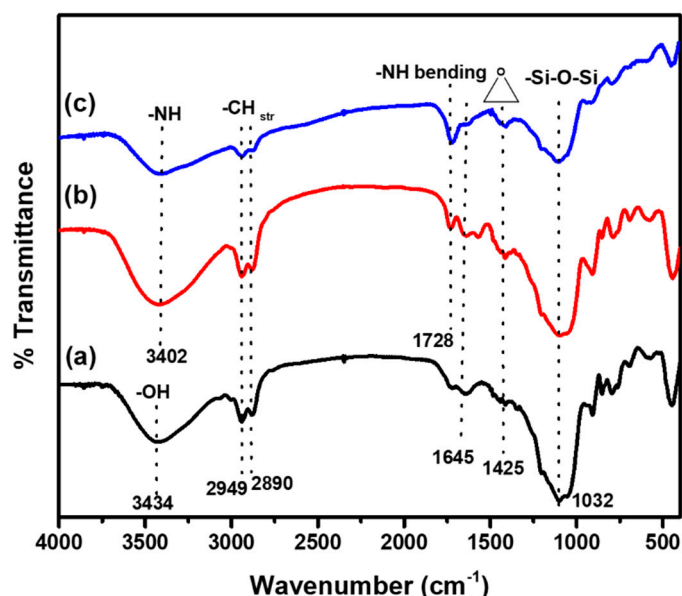


**Figure 1.** Fourier transform infrared (FT-IR) spectra of (a) Hy-coated, (b) Hy/chitosan-coated, and (c) Hy/chitosan/3-mercaptopropionic acid (MPA)-coated Cu electrodes.

#### 3.2. X-ray Photoelectron Spectroscopy (XPS) Analysis

The XPS spectra shown in Figure 2 were used to determine the chemical composition of bare Cu, Hy coated, Hy/chitosan coated, and Hy/chitosan/MPA coated Cu electrodes. The peaks of bare Cu shows three peaks at 497.7, 933.6, and 952.5 eV due to the presence of O 1s, Cu  $2p_{3/2}$ , and Cu  $2p_{1/2}$ , respectively. For the Hy-coated electrode, the peaks are shown at 104.6, 153.6, 286.1, 534.1, and 980.1 eV due to the presence of Si 2s, Si 2p, C 1s, O 1s, and Cu  $2p_{3/2}$ , which confirm the presence of the hybrid sol-gel coating on copper surface. The peaks of Hy/chitosan coated electrode are shown at 122.2, 162.5, 283.4, 496.3, 534.1, 933.6, and 980.1 eV due to the presence of Si 2s, Si 2p, C 1s, N 1s, O 1s, Cu  $2p_{3/2}$ , and Cu  $2p_{1/2}$ , confirming the doping of chitosan in the hybrid sol-gel matrix. Furthermore, the Hy/chitosan/MPA-coated electrode shows peaks at 99.6, 153.6, 162.5, 284.7, 400.5, 531.6, and 977.6 eV due to the presence of Si 2s, Si 2p, S 2p, C 1s, N 1s, O 1s, and Cu  $2p_{3/2}$ . The expanded XPS spectrum of the Hy-coated electrode (Figure 3) shows C 1s peaks consisting of three binding peaks at 284.7, 286.3, and 288.2 eV due to the presence of  $\text{C-C}$ ,  $\text{C-O-C}$ , and  $\text{C-OH}$  functional groups. The XPS of O 1s level shows two binding peaks at 532.4 eV and 533.1 eV due to the presence of  $\text{C-O-C}$  and  $\text{Si-O}$  functional groups. The XPS spectrum of Si 2p shows one binding peaks at 102.8 eV due to the presence of  $\text{Si-O-Si}$  bond formation confirming the hydrolysis and condensation reaction of coated hybrid sol-gel on the Cu metal [26].

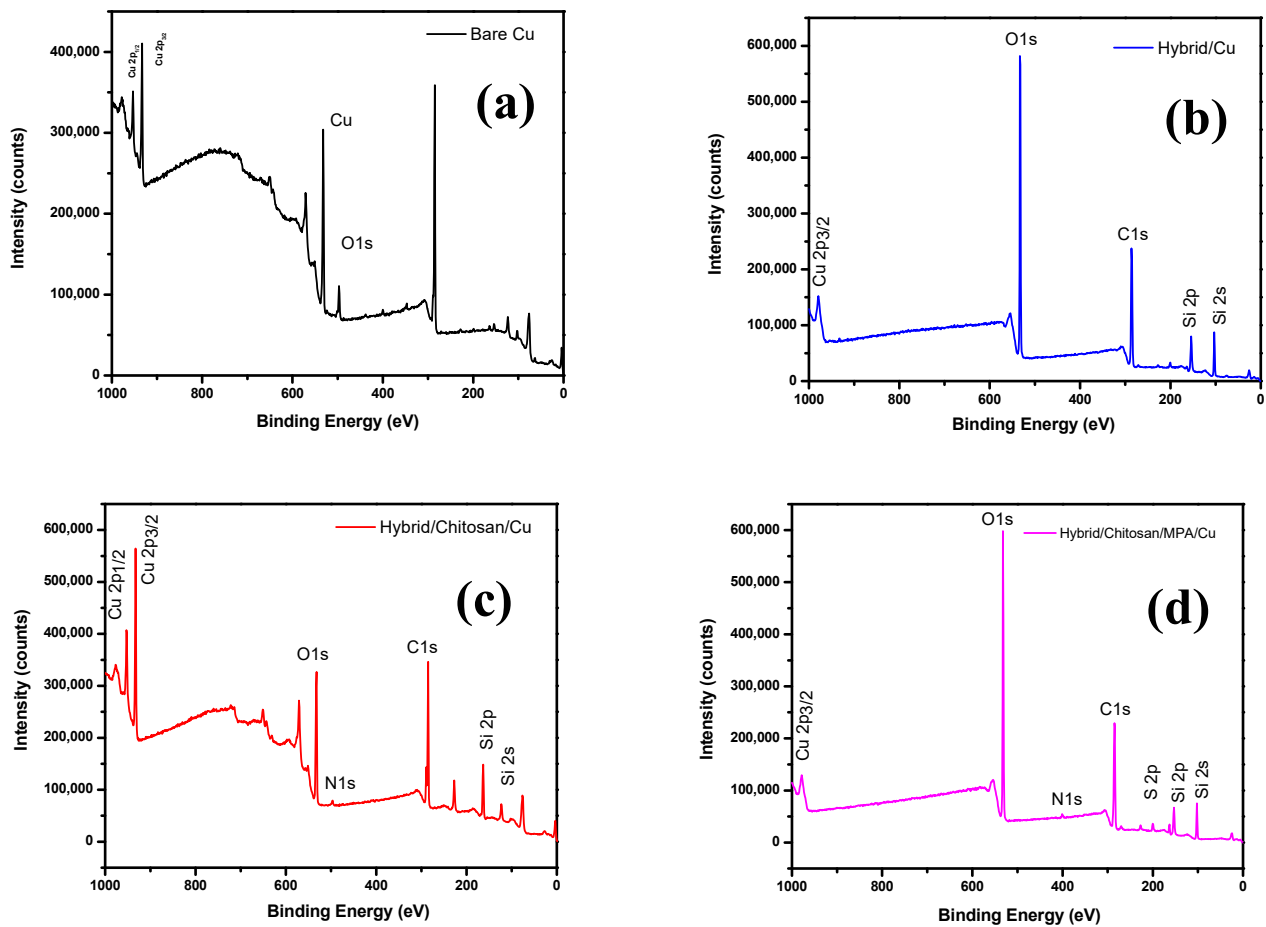


**Figure 2.** X-ray photoelectron spectroscopy (XPS) spectra of (a) bare Cu, (b) Hy-coated, (c) Hy/chitosan-coated, and (d) Hy/chitosan/MPA-coated Cu electrodes.

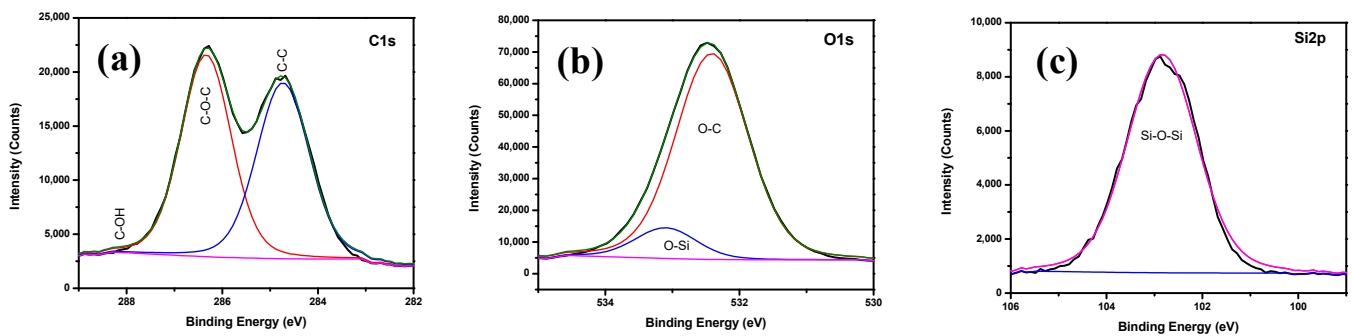


**Figure 3.** Deconvoluted XPS spectra of Hy-coated Cu electrodes; (a) C 1s, (b) O 1s, and (c) Si 2p.

The expanded XPS spectrum of Hy/chitosan-coated (Figure 4) shows C 1s peaks consisting of four binding peaks at 284.7, 286.1, 287.9, and 288.9 eV due to the presence of C–N, C–C, C–O–C, and C–OH functional groups. The O 1s level shows two binding peaks at 531.8 and 533.3 eV due to the presence of C–O–C and Si–O groups. The Si 2p shows one binding peak at 102.8 eV due to the presence of Si–O–Si bond formation. The N 1s shows one binding peaks at 399.9 eV due to the presence of C–N bond formation confirming the doping of chitosan into the hybrid sol-gel matrix and the coating on Cu metal.

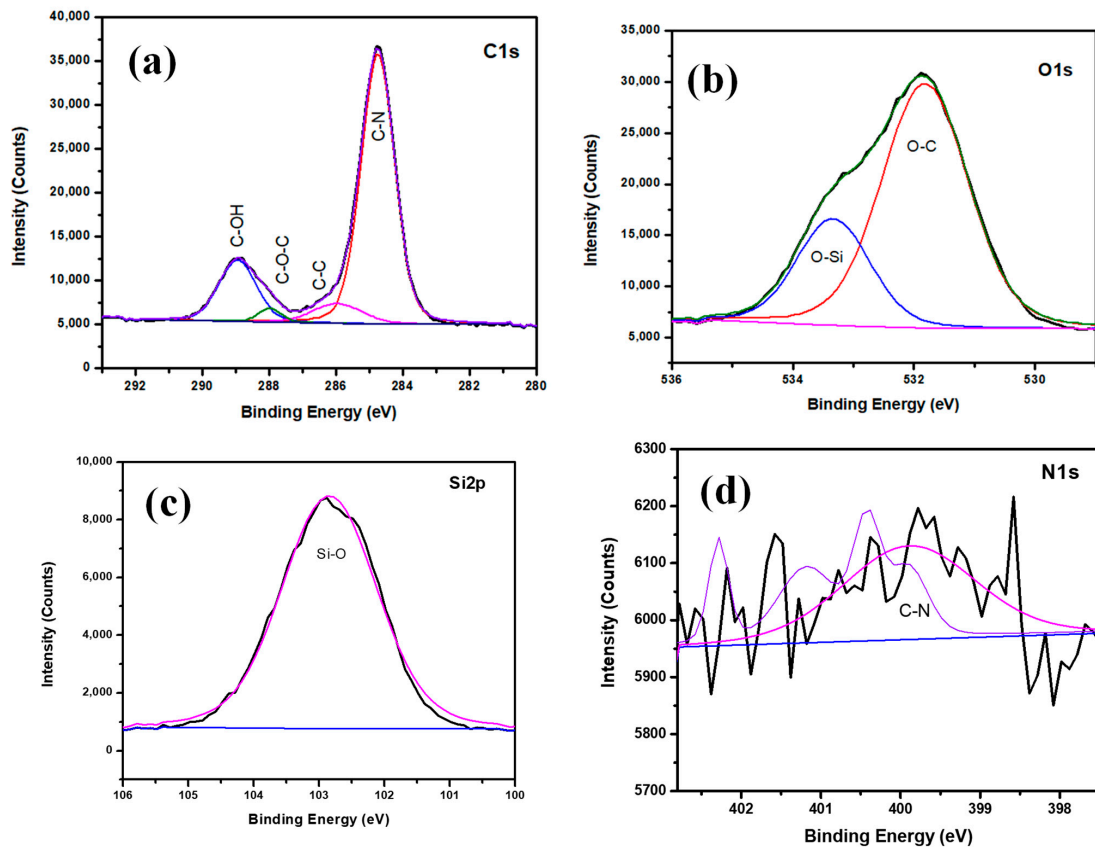


Figure 4. Deconvoluted XPS spectra of Hy/chitosan coated electrodes; (a) C 1s, (b) O 1s, (c) Si 2p, and (d) N 1s.

In the expanded XPS spectrum of Hy/chitosan/MPA-coated electrode (Figure 5), similar peaks to those of Hy/chitosan-coated electrodes are shown and additionally, the peak of S 2p is shown for one binding peaks at 163.1 eV due to the presence of Cu–S (thiolate bond) formation, confirming the doping of MPA into Hy/chitosan sol-gel matrix and the coating on Cu metal.

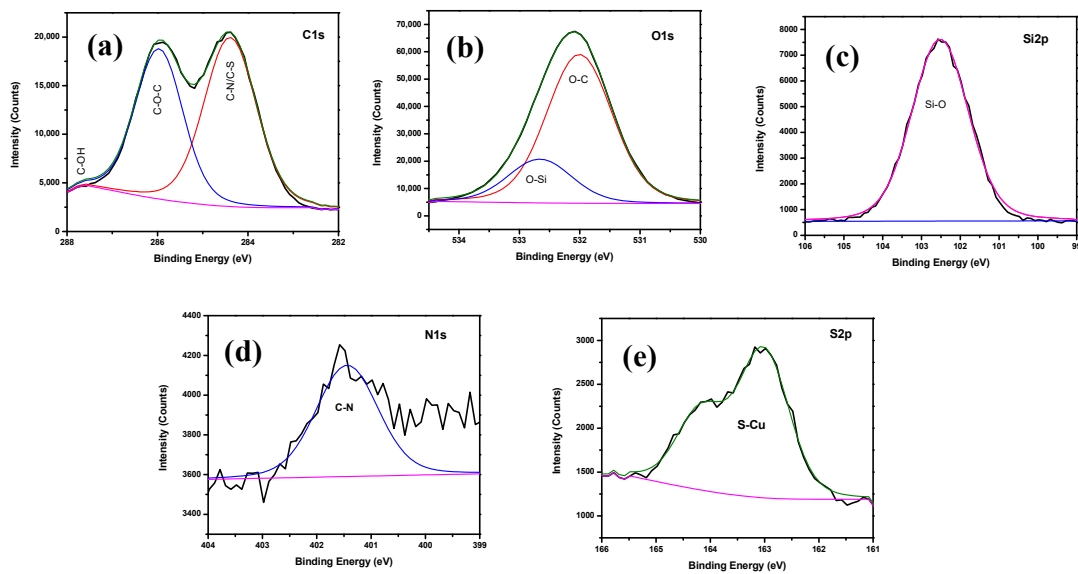
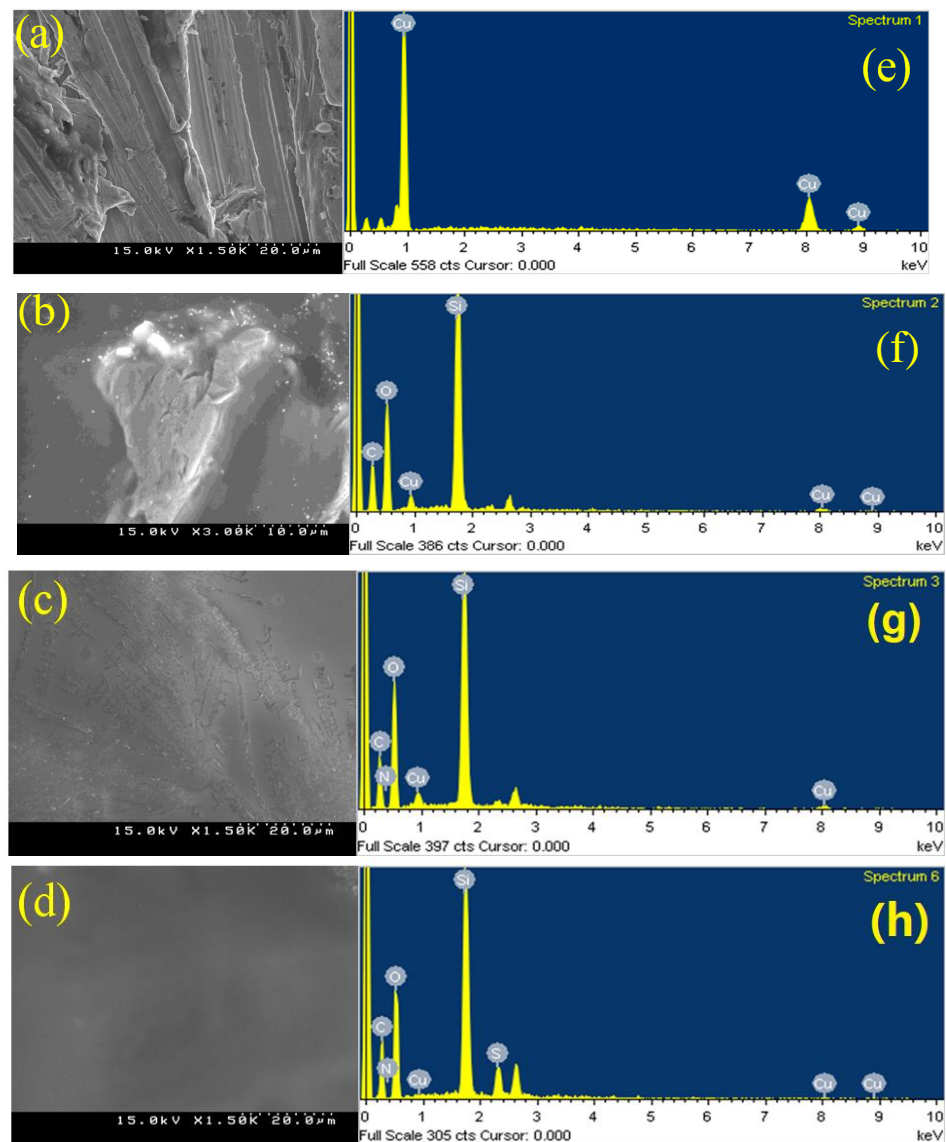


Figure 5. Deconvoluted XPS spectra of Hy/chitosan/MPA coated electrodes; (a) C 1s (b) O 1s (c) Si 2p (d) N 1s and (e) S 2p.

The calculated atomic weights (%) for Hy/chitosan/MPA sol-gel are C (47.6%), O (37.97%), Si (11.64%), N (1.37%), S (1.33%), and Cu (0.09%) [10]. The XPS analysis confirmed the formation of an MPA/chitosan/Hybrid sol-gel layer on the Cu metal.

### 3.3. Scanning Electron Microscopy (SEM) and Energy-Dispersive X-ray Spectroscopy (EDX) Analysis

The SEM photographs for the bare Cu, Hy coated, Hy/chitosan coated, and Hy/chitosan/MPA coated Cu electrodes are presented in Figure 6a–d, respectively. The SEM image of bare Cu (Figure 6a) shows a lot of scratches due to polishing the Cu surfaces, while Hy coated electrode (Figure 6b) shows a poor adhesive layer on the Cu metal due to unstable Cu–O–Si bond formation [10,21,25,27]. Hy/chitosan-coated (Figure 6c) electrode shows uniform distribution of chitosan layer. The hybrid sol-gel coated and Hy/chitosan/MPA-coated Cu electrodes show (Figure 6d) a dense and compactly packed adhesive layer that can protect the copper metal from corrosion.



**Figure 6.** Scanning electron microscopy (SEM) images and energy-dispersive X-ray spectroscopy (EDX) of bare Cu (a,e), Hy coated (b,f), Hy/chitosan coated (c,g), and Hy/chitosan/MPA coated Cu electrodes (d,h).

The EDAX results for the bare Cu, Hy-coated, Hy/chitosan-coated, and Hy/chitosan/MPA-coated Cu electrodes are shown in Figure 6e–h, respectively. In bare Cu (Figure 6e) the peaks at 1, 8 and 9 keV for Cu metal, while the Hy-coated (Figure 6f) electrode shows peaks at 0.25, 0.50, 1.0, and 1.8 keV due to presence of C, O, Cu and Si confirming the coating of hybrid sol-gel. In the Hy/chitosan-coated electrode (Figure 6g), the additional peak of N at 0.30 keV is shown, confirming the doping of chitosan into a hybrid sol-gel matrix. For the MPA with Hy/chitosan sol-gel, a new additional peak of S at 2.15 keV is shown, confirming the doping of MPA and the forming a protective layer on Cu metal.

### 3.4. Atomic Force Microscopy (AFM) Analysis

The AFM images of bare Cu and Hy/chitosan/MPA-coated Cu electrodes are shown in Figure 7. The bare Cu shows scratches same as the SEM image. For the Hy/chitosan/MPA-coated Cu electrode (Figure 7b), a uniform adhering layer is shown. Average surface roughness ( $S_a$ ) and root mean square ( $S_q$ ) of the Hy/Chitosan/MPA-coated electrode are lower than those of bare Cu (Table 1). The decrease in surface roughness of Hy/Chitosan/MPA-coated Cu indicates the formation of a densely packed layer on the Cu metal [27].

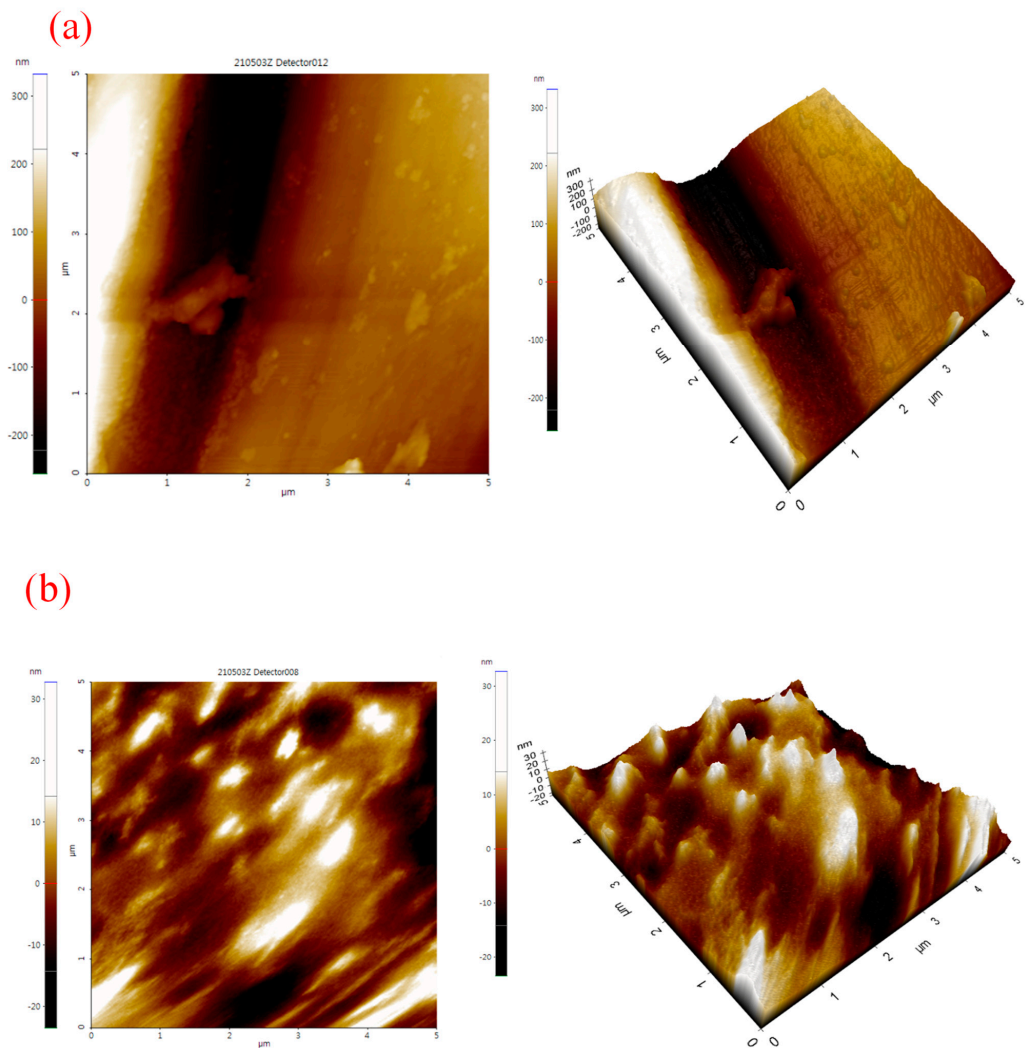


**Figure 7.** Atomic force microscopy (AFM) images of (a) bare Cu and (b) Hy/chitosan/MPA-coated Cu electrode.

**Table 1.** AFM roughness parameters (nm) for (a) bare Cu and (b) Hy/chitosan/MPA-coated Cu electrodes.

Nature of Sol-Gel Coating	Average Surface Roughness (Sa) (nm)	Root Mean Square (Sq) (nm)
Bare Cu	123.4	146.0
Hy/Chitosan/MPA/Cu	4.6	6.2

### 3.5. Electrochemical Impedance Spectroscopy (EIS)

EIS for Cu metal, Hy-coated, Hy/chitosan-coated, and Hy/chitosan/MPA-coated Cu electrodes was analyzed after immersing them in 3.5% NaCl solution for 1 h and the corresponding Nyquist plot is shown in Figure 8. The results were fitted using an equivalent circuit shown in Figure 9 and the fitted parameters are shown in Table 2. In the equivalent circuit for bare Cu (Figure 9a),  $R_s$  is the solution resistance,  $R_{ct}$  the charge transfer resistance,  $W$  the Warburg impedance, and  $Q_{dl}$  the double layer capacitance, respectively. For sol-gel modified Cu (Figure 9b),  $R_{sam}$  and  $Q_{sam}$  are coated resistance and coated double layer capacitance, respectively [10].

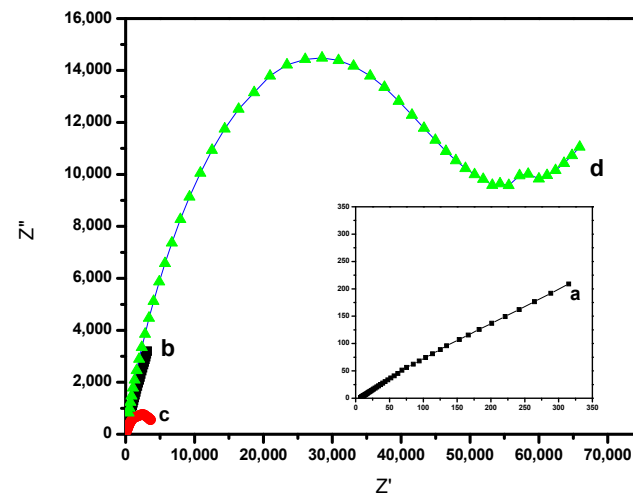


**Figure 8.** Electrochemical impedance spectroscopy (EIS) of (a) bare Cu (inset), (b) Hy-coated, (c) Hy/chitosan-coated, and (d) Hy/chitosan/MPA-coated Cu electrodes in 3.5% NaCl solution.

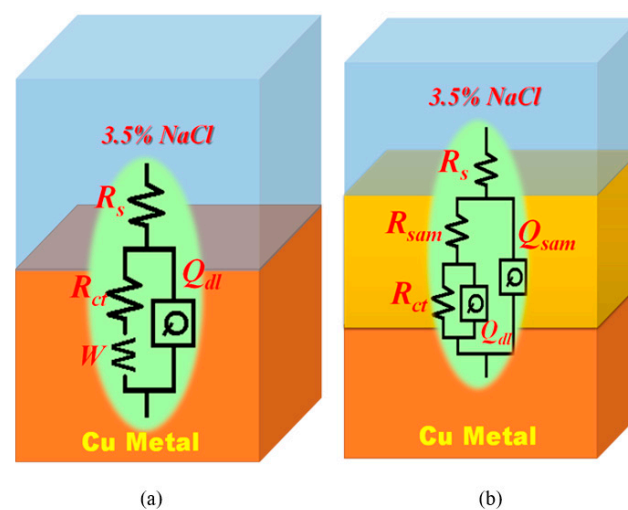


**Figure 9.** Equivalent circuits of (a) bare Cu and (b) coated Cu substrates.

**Table 2.** Electrochemical impedance parameters for bare Cu, Hy-coated, Hy/chitosan-coated, and Hy/chitosan/MPA-coated Cu electrodes in 3.5% NaCl solution.

Nature of Sol-Gel Coatings	$-E_{corr}$ (mV)	$i_{corr}$ ( $\mu\text{A}\cdot\text{cm}^{-2}$ )	$\eta_{PDS}$ (%)
Bare Cu	−292	$7.09 \times 10^{-4}$	-
Hy/Cu	−222	$1.18 \times 10^{-4}$	83.3
Hy/Chitosan/Cu	−215	$7.05 \times 10^{-5}$	90.0
Hy/Chitosan/MPA/Cu	−165	$4.08 \times 10^{-7}$	99.9

The corrosion protection efficiency of bare Cu and modified Cu electrodes in the EIS analysis were calculated using Equation (1) [28].

$$IE(EIS)(\%) = \frac{R_{ct}^s - R_{ct}^b}{R_{ct}^b} \times 100 \quad (1)$$

where,  $R_{ct}^s$  and  $R_{ct}^b$  are the charge transfer resistance of the modified and unmodified Cu electrodes, respectively.

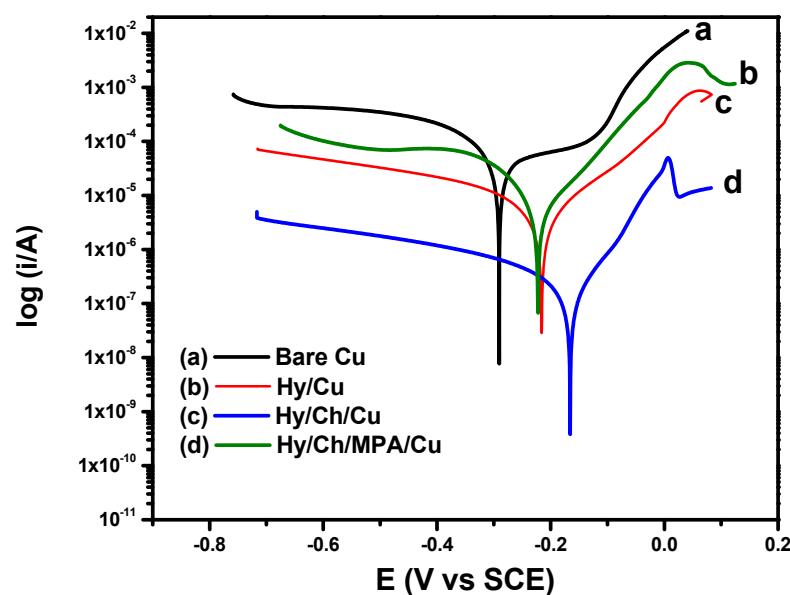
The Hy/chitosan/MPA-coated Cu electrode shows the largest  $R_{ct}^s$  values compared to bare Cu, Hy-coated, and Hy/chitosan-coated layers, and hence the Hy/chitosan/MPA-coated Cu electrode showed the highest corrosion inhibition efficiency of 99.9%. The Hy/chitosan/MPA acts as a very good protective layer against the diffusion of corrosive chloride ions into Cu metal surface.

### 3.6. Potentiodynamic Polarization Studies (PDS)

From PDS analysis, the corresponding Tafel plot is shown in Figure 10 and the Tafel parameters are summarized in Table 3. The corrosion inhibition efficiency for unmodified and modified Cu electrodes in the Tafel plot were calculated using Equation (2) [29,30].

$$IE(PDS)(\%) = \frac{i_{corr}^b - i_{corr}^s}{i_{corr}^b} \times 100 \quad (2)$$

where,  $i_{corr}^b$  and  $i_{corr}^s$  are the corrosion current of the unmodified and modified Cu metals, respectively.

**Figure 10.** Potentiodynamic study(PDS) of (a) bare Cu, (b) Hy-coated, (c) Hy/chitosan-coated, and (d) Hy/chitosan/MPA-coated Cu electrodes in 3.5% NaCl solution.

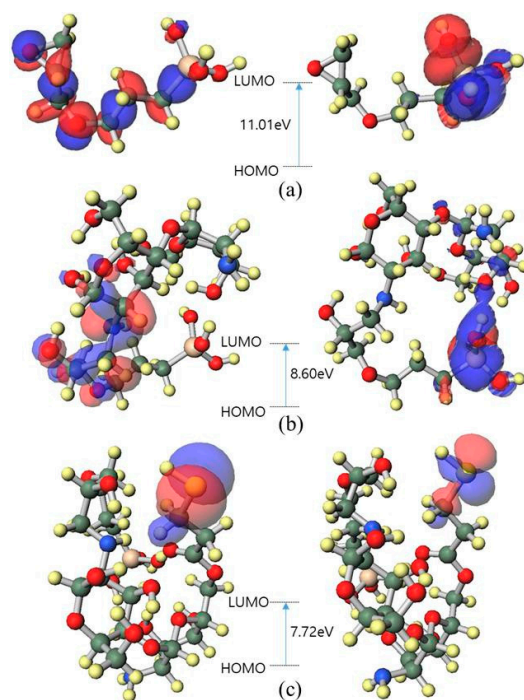
**Table 3.** Tafel parameters for (a) bare Cu, (b) Hy-coated, (c) Hy/chitosan-coated, and (d) Hy/chitosan/MPA-coated Cu electrodes in 3.5% NaCl solution.

Parameters	Bare Cu	Hy/Cu	Hy/Chitosan/Cu	Hy/Chitosan/MPA/Cu
$R_s$ ( $\Omega$ )	5.0	6.2	9.0	10.0
$Q_{sam}$ ( $\mu\text{F cm}^{-2}$ )	-	$2.25 \times 10^{-5}$	$1.01 \times 10^{-5}$	$3.11 \times 10^{-7}$
$n_1$	-	0.70	0.80	0.73
$R_{sam}$ ( $\Omega \text{ cm}^2$ )	-	30.5	48.3	76.2
$Q_{dl}$ ( $\mu\text{F cm}^{-2}$ )	$1.17 \times 10^{-3}$	$1.68 \times 10^{-5}$	$1.53 \times 10^{-5}$	$1.55 \times 10^{-5}$
$n_2$	0.80	0.80	0.53	0.85
$R_t$ ( $\text{k}\Omega$ )	586.4	3557	6256	9,764,000
$\eta$ (%) using $R_t$	-	83.5	90.6	99.9

The further decrease in  $i_{corr}^s$  value for Hy/chitosan/MPA-coated Cu electrodes was observed due to doping of MPA and chitosan with extended silane linkages. Hy/chitosan/MPA-coated Cu electrodes shows extended anodic shifts compared to Hy/Cu- and Hy/chitosan sol-gel coated electrodes. Hy/chitosan/MPA coating protects the Cu electrodes against anodic oxidation reaction and the formation of an adhesive barrier layer against the attack of aggressive chloride ions [21,27].

### 3.7. Mechanism

Density functional theory (DFT) was computed using a semi-empirical molecular orbital package (MOPAC) with PM7 Hamiltonian. The highest occupied molecular orbital (HOMO) energy and the lowest unoccupied molecular orbital (LUMO) energy were calculated and are presented in Figure 11. The energy of the Hy/chitosan/MPA is the smallest value of 7.72 eV. The more stable inhibitor with a lower HOMO-LUMO gap energy leads to a higher corrosion efficiency [31]. A higher HOMO energy level reduces the HOMO-LUMO gap energy and induces organic molecules to give free electrons to the metal surface, resulting in a high inhibition efficiency.

**Figure 11.** Highest occupied molecular orbital (HOMO) and lowest unoccupied molecular orbital (LUMO) band gap energy of (a) Hy-coated, (b) Hy/chitosan-coated, and (c) Hy/chitosan/MPA-coated, respectively.

The schematic representation of Hy/chitosan/MPA sol-gel coated layer on Cu metal is shown in Figure 12. The acidic carbon in the hybrid sol-gel undergoes nucleophilic attack by the addition of chitosan biopolymer leading to the opening of the epoxy ring and the formation of the Si–O–Si linkage. The addition of 3-mercaptopropionic acid (MPA) to chitosan/hybrid sol-gel induces an addition reaction by the elimination of water. This sol-gel matrix was grafted onto Cu metal by a self-assembly method leading to the formation of a Cu–S (thiolate) bond. Thus, the MPA-doped chitosan/Hy sol-gel layer protects the Cu metal from corrosion in a 3.5% NaCl solution [32,33].

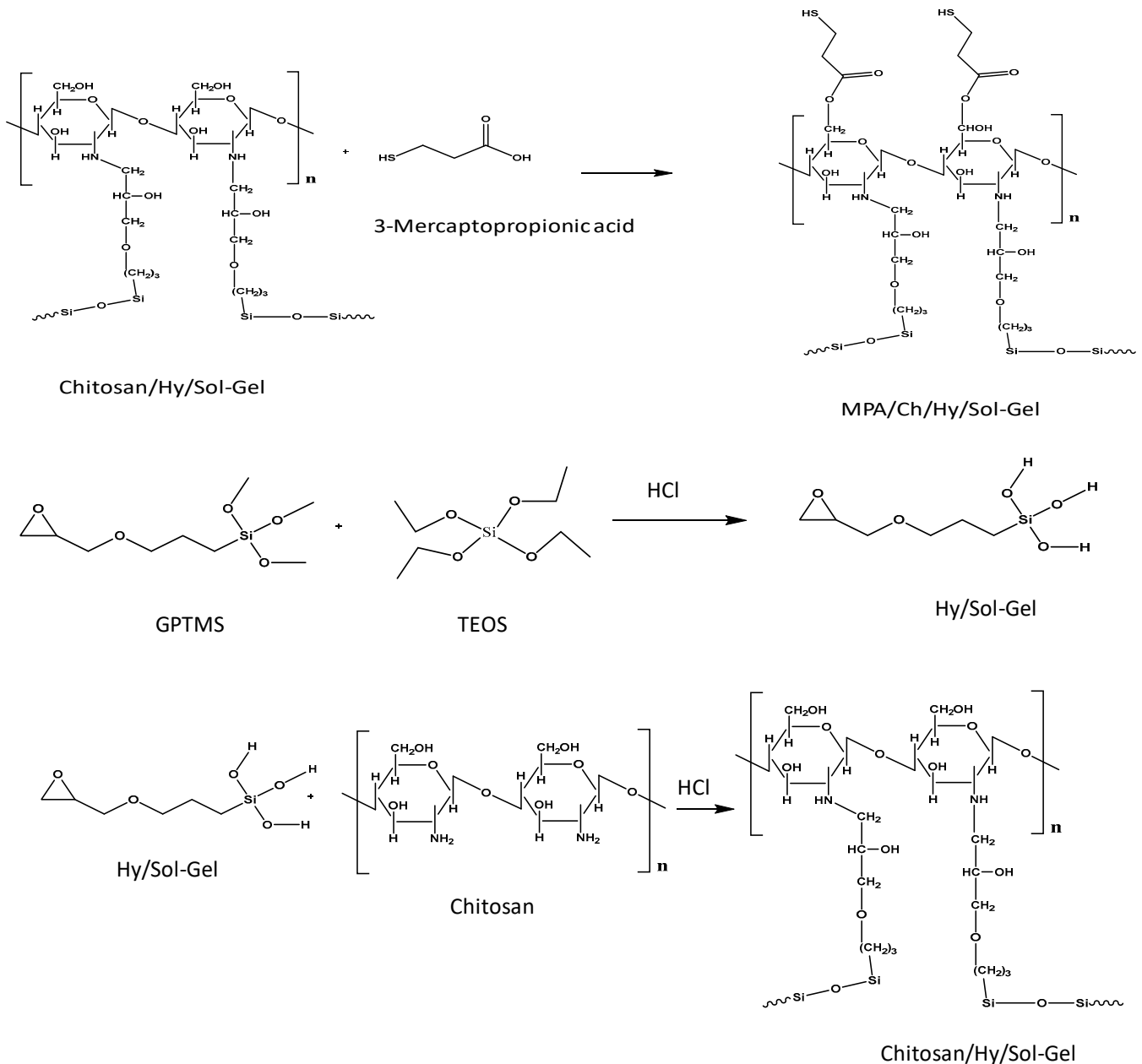
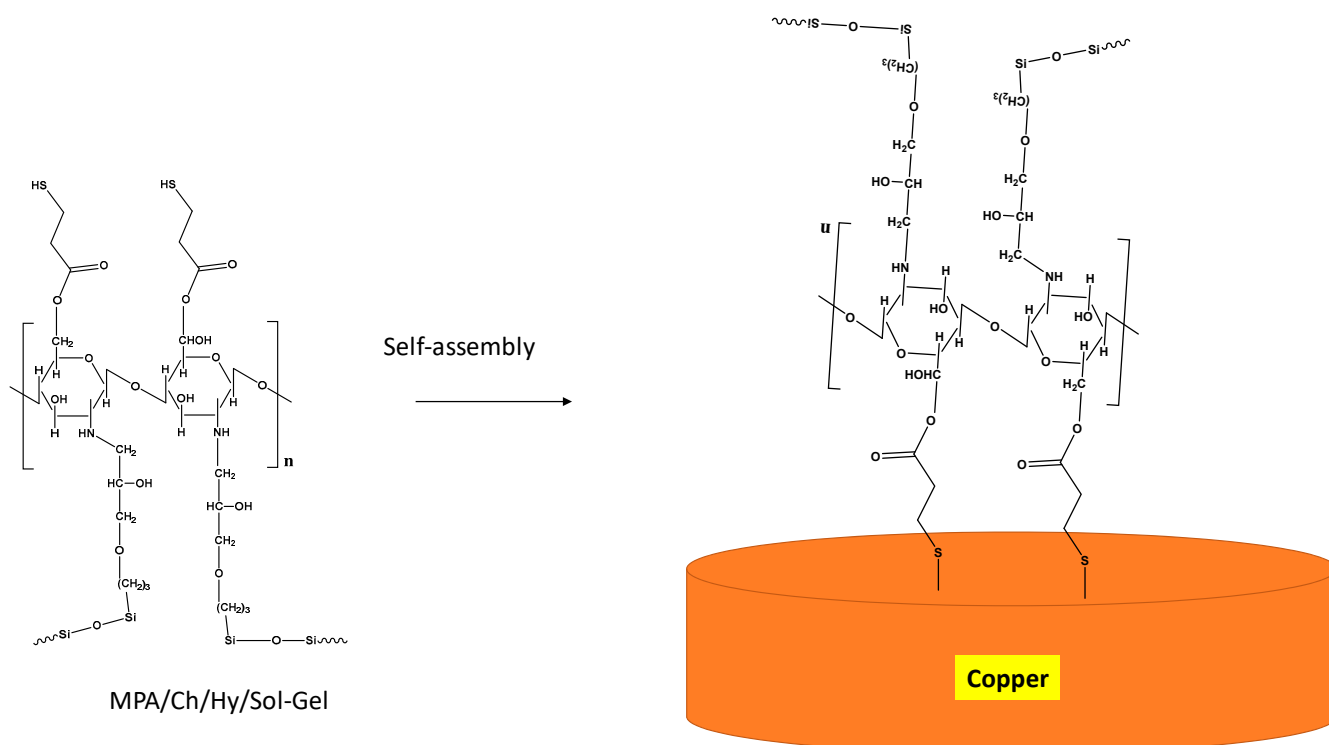


Figure 12. Cont.



**Figure 12.** Proposed mechanism of Hy/chitosan/MPA sol-gel coating on Cu metal.

#### 4. Conclusions

Chitosan biopolymer based sol-gel doping with 3-mercaptopropanoic acid (MPA) and hybrids is a successful strategy to protect Cu metal surface. Chemical composition analyses like FT-IR and XPS revealed the formation of Si–O–Si, Cu–S, and epoxy ring opening, confirming the doping of chitosan biopolymer and MPA to the hybrid sol-gel matrix. SEM and AFM analyses confirmed the formation of an adhesive homogenous layer of Hy/chitosan/MPA sol-gel coated layer on Cu metal. The EIS and PDS results showed that the corrosion inhibition efficiency of an MPA-doped chitosan/Hy sol-gel coated layer is 99.9%. A very high corrosion inhibition of the MPA-doped chitosan/Hy sol-gel coated layer was achieved, and it can be used in industrial application to protect Cu metal in a NaCl solution.

**Author Contributions:** J.B.: Conceptualization, Methodology, Data curation, Software, Writing—Original draft, Visualization, Editing. T.H.O.: Reviewing, Supervision. All authors have read and agreed to the published version of the manuscript.

**Funding:** This work was supported by the National Research Foundation of Korea (NRF) grant funded by the Korean government (MSIT) (2020R1A2C1005959).

**Conflicts of Interest:** The authors declare no conflict of interest.

#### References

- Bao, Q.; Zhang, D.; Wan, Y. 2-Mercaptobenzothiazole doped chitosan/11-alkanethiolate acid composite coating: Dual function for copper protection. *Appl. Surf. Sci.* **2011**, *257*, 10529–10534. [[CrossRef](#)]
- Rao, B.A.; Iqbal, M.Y.; Sreedhar, B. Self-assembled monolayer of 2-(octadecylthio) benzothiazole for corrosion protection of copper. *Corros. Sci.* **2009**, *5*, 1441–1452.
- Vera, R.; Bastidas, F.; Villarroel, M.; Oliva, A.; Molinari, A.; Ramírez, D.; del Rio, R. Corrosion inhibition of copper in chloride media by 1, 5-bis (4-dithiocarboxylate-1-dodecyl-5-hydroxy-3-methylpyrazolyl) pentane. *Corros. Sci.* **2008**, *50*, 729–736. [[CrossRef](#)]
- Fonder, G.; Laffineur, F.; Delhalle, J.; Mekhalif, Z. Alkanethiol-oxidized copper interface: The critical influence of concentration. *J. Colloid Interface Sci.* **2008**, *326*, 333–338. [[CrossRef](#)]
- Nurioglu, A.G.; Esteves, A.C. Non-toxic, non-biocide-release antifouling coatings based on molecular structure design for marine applications. *J. Mater. Chem. B* **2015**, *3*, 6547–6570. [[CrossRef](#)]

6. Pareek, S.; Jain, D.; Hussain, S.; Biswas, A.; Shrivastava, R.; Parida, S.K.; Kisan, H.K.; Lgaz, H.; Chung, I.M.; Behera, D. A new insight into corrosion inhibition mechanism of copper in aerated 3.5 wt.% NaCl solution by eco-friendly Imidazopyrimidine Dye: Experimental and theoretical approach. *Chem. Eng. J.* **2019**, *358*, 725–742. [[CrossRef](#)]
7. Hamidon, T.S.; Hussin, M.H. Susceptibility of hybrid sol-gel (TEOS-APTES) doped with caffeine as potent corrosion protective coatings for mild steel in 3.5 wt.% NaCl. *Prog. Org. Coat.* **2020**, *140*, 105478. [[CrossRef](#)]
8. Daubert, J.S.; Hill, G.T.; Gotsch, H.N.; Gremaud, A.P.; Ovental, J.S.; Williams, P.S.; Oldham, C.J.; Parsons, G.N. Corrosion protection of copper using Al<sub>2</sub>O<sub>3</sub>, TiO<sub>2</sub>, ZnO, HfO<sub>2</sub>, and ZrO<sub>2</sub> atomic layer deposition. *ACS Appl. Mater. Interfaces* **2017**, *9*, 4192–4201. [[CrossRef](#)] [[PubMed](#)]
9. Figueira, R.B.; Silva, C.J.; Pereira, E.V. Organic–inorganic hybrid sol–gel coatings for metal corrosion protection: A review of recent progress. *J. Coat. Technol. Res.* **2015**, *12*, 1–35. [[CrossRef](#)]
10. Balaji, J.; Roh, S.H.; Edison, T.N.; Jung, H.Y.; Sethuraman, M.G. Sol-gel based hybrid silane coatings for enhanced corrosion protection of copper in aqueous sodium chloride. *J. Mol. Liq.* **2020**, *302*, 112551. [[CrossRef](#)]
11. Asadi, N.; Naderi, R.; Saremi, M.; Arman, S.Y.; Fedel, M.; Deflorian, F. Study of corrosion protection of mild steel by eco-friendly silane sol–gel coating. *J. Sol Gel Sci. Technol.* **2014**, *70*, 329–338. [[CrossRef](#)]
12. Zheludkevich, M.L.; Salvado, I.M.; Ferreira, M.G. Sol-gel coatings for corrosion protection of metals. *J. Mater. Chem.* **2005**, *15*, 5099–5111. [[CrossRef](#)]
13. Samiee, R.; Ramezanzadeh, B.; Mahdavian, M.; Alibakhshi, E. Assessment of the smart self-healing corrosion protection properties of a water-base hybrid organo-silane film combined with non-toxic organic/inorganic environmentally friendly corrosion inhibitors on mild steel. *J. Clean. Prod.* **2019**, *220*, 340–356. [[CrossRef](#)]
14. Kumar, M.N. A review of chitin and chitosan applications. *React. Funct. Polym.* **2000**, *46*, 1–27. [[CrossRef](#)]
15. Balaji, J.; Sethuraman, M.G. Chitosan-doped-hybrid/TiO<sub>2</sub> nanocomposite based sol-gel coating for the corrosion resistance of aluminum metal in 3.5% NaCl medium. *Int. J. Biol. Macromol.* **2017**, *104*, 1730–1739.
16. Balaji, J.; Raja, P.B.; Sethuraman, M.G.; Oh, T.H. Experimental and multiscale simulation studies on Chitosan doped Hybrid/Zirconium—A bio-nanocomposite coating for aluminium protection. *J. Sol Gel Sci. Technol.* **2021**, 1–11. [[CrossRef](#)]
17. Ruhi, G.; Modi, O.P.; Dhawan, S.K. Chitosan-polypyrrole-SiO<sub>2</sub> composite coatings with advanced anticorrosive properties. *Synth. Met.* **2015**, *200*, 24–39. [[CrossRef](#)]
18. Carneiro, J.; Tedim, J.; Fernandes, S.C.; Freire, C.S.; Gandini, A.; Ferreira, M.G.; Zheludkevich, M.L. Functionalized chitosan-based coatings for active corrosion protection. *Surf. Coat. Technol.* **2013**, *226*, 51–59. [[CrossRef](#)]
19. Laibinis, P.E.; Whitesides, G.M. Self-assembled monolayers of n-alkanethiolates on copper are barrier films that protect the metal against oxidation by air. *J. Am. Chem. Soc.* **1992**, *114*, 9022–9028. [[CrossRef](#)]
20. Álvarez, D.; Collazo, A.; Hernández, M.; Nóvoa, X.R.; Pérez, C. Characterization of hybrid sol–gel coatings doped with hydrotalcite-like compounds to improve corrosion resistance of AA2024-T3 alloys. *Prog. Org. Coat.* **2010**, *68*, 91–99. [[CrossRef](#)]
21. Karthik, N.; Sethuraman, M.G. Improved copper corrosion resistance of epoxy-functionalized hybrid sol–gel monolayers by thiosemicarbazide. *Ionics* **2015**, *21*, 1477–1488. [[CrossRef](#)]
22. Balgude, D.; Konge, K.; Sabnis, A. Synthesis and characterization of sol–gel derived CNSL based hybrid anti-corrosive coatings. *J. Sol Gel Sci. Technol.* **2014**, *69*, 155–165. [[CrossRef](#)]
23. Purcar, V.; Şomoghi, R.; Niţu, S.G.; Nicolae, C.A.; Alexandrescu, E.; Gifu, I.C.; Gabor, A.R.; Stroescu, H.; Ianchiş, R.; Căprărescu, S.; et al. The effect of different coupling agents on nano-ZnO materials obtained via the sol–gel process. *Nanomaterials* **2017**, *7*, 439. [[CrossRef](#)] [[PubMed](#)]
24. Ma, S.; Liu, W.; Wei, Z.; Li, H. Mechanical and thermal properties and morphology of epoxy resins modified by a silicon compound. *J. Macromol. Sci. A* **2010**, *47*, 1084–1090. [[CrossRef](#)]
25. Balaji, J.; Sethuraman, M.G. Corrosion protection of copper with hybrid sol-gel containing 1H-1, 2, 4-triazole-3-thiol. *Iran. J. Chem. Chem. Eng.* **2016**, *35*, 61–71.
26. Milošev, I.; Jovanović, Ž.; Bajat, J.B.; Jančić-Heinemann, R.; Mišković-Stanković, V.B. Surface analysis and electrochemical behavior of aluminum pretreated by vinyltriethoxysilane films in mild NaCl solution. *J. Electrochem. Soc.* **2012**, *159*, C303. [[CrossRef](#)]
27. Karthik, N.; Asha, S.; Sethuraman, M.G. Influence of pH-sensitive 4-aminothiophenol on the copper corrosion inhibition of hybrid sol–gel monolayers. *J. Sol Gel Sci. Technol.* **2016**, *78*, 248–257. [[CrossRef](#)]
28. Ziat, Y.; Abbas, N.; Hammi, M.; Echihi, S. An experimental evaluation of inhibiting corrosion effect of phosphate glass on mild steel in acidic solution. *Mater. Res. Express.* **2019**, *6*, 086567. [[CrossRef](#)]
29. Tan, B.; Xiang, B.; Zhang, S.; Qiang, Y.; Xu, L.; Chen, S.; He, J. Papaya leaves extract as a novel eco-friendly corrosion inhibitor for Cu in H<sub>2</sub>SO<sub>4</sub> medium. *J. Colloid Interface Sci.* **2021**, *582*, 918–931. [[CrossRef](#)]
30. Tan, B.; He, J.; Zhang, S.; Xu, C.; Chen, S.; Liu, H.; Li, W. Insight into anti-corrosion nature of Betel leaves water extracts as the novel and eco-friendly inhibitors. *J. Colloid Interface Sci.* **2020**, *585*, 287–301. [[CrossRef](#)]
31. Fang, J.; Li, J. Quantum chemistry study on the relationship between molecular structure and corrosion inhibition efficiency of amides. *J. Mol. Struct. THEOCHEM* **2002**, *593*, 179–185. [[CrossRef](#)]
32. Balaji, J.; Sethuraman, M.G. Corrosion protection of copper with 3-glycidoxypropyltrimethoxysilane-based sol–gel coating through 3-amino-5-mercapto-1, 2, 4-triazole doping. *Res. Chem. Intermed.* **2016**, *42*, 1315–1328. [[CrossRef](#)]
33. Innocenzi, P.; Kidchob, T.; Yoko, T. Hybrid organic-inorganic sol-gel materials based on epoxy-amine systems. *J. Sol Gel Sci. Technol.* **2005**, *35*, 225–235. [[CrossRef](#)]